An Analysis of Carrier-Based Multilevel Modulation Strategies with Different Carrier Dispositions Applied to an Open-End Winding Power Converter

Hugo R. Torquato, Herbert O. Ramos, Frederico F. V. Matos and Clodualdo V. Sousa, Victor F. Mendes
Technological Sciences Institute
Federal University of Itajubá
Itabira, Brasil
hugortorquato@gmail.com, herbert-ramos11@ufmg.br, frederico.matos@unifei.edu.br, clodualdosousa@unifei.edu.br, victormendes@cpde

***Abstract*—This paper presents an analysis of multilevel pulse width modulation techniques using different carrier dispositions applied to a three-level open-end-winding configuration. The structure uses a pair of two-level back-to-back converters, and the studied carrier dispositions were the Phase Shifted (PS), Level Shifted with Phase Disposition (PD) and Phase Opposition Disposition (POD). Techniques were implemented in an experimental setup and analysis was performed based on the spectral content of the resulting voltages and currents. Finally, the total harmonic distortion was calculated from the data for the entire modulation range allowing for a proper comparison between strategies, evidencing the superior performance of the Phase Disposition technique.**

***Index Terms*—Multilevel Converters, Open-End Winding, Multilevel Modulation Techniques.**

I. Introduction

Static power converters can be applied to several different processes and applications. Over the years, the increasing demand for higher energy ratings, power quality and reliability has pushed power electronics devices towards their operational limits. This demand motivated the development of materials, topologies and control techniques. In this context, multilevel converters have gained popularity and configurations such as the Neutral Point Clamped (NPC), Flying Capacitor (FC), Cascaded H-Bridge (CHB) and Modular Multilevel Converters (MMC) have become products with high acceptance [1].

This work presents a comparative study of modulation techniques employing distinct carrier dispositions for a three-level open-end winding (OEW) conversion system. The OEW configuration was introduced by [2], and consists of connecting static converters to both ends of poly-phase windings, as depicted in Fig. 1, instead of the traditional Δ/Y connection.

This topology presents the same voltage outputs as the traditional three-level systems, such as NPC and FC, but with no clamping diodes nor flying capacitors. Its main restriction, however, is the need for isolation between the converters in order to avoid common-mode circulating currents. OEW systems have been reported for several applications, such as microgrid [4], electrical vehicles [5] and wind power [6], to name a few.

The authors would like to thank the Brazilian agencies CAPES, FAPEMIG and CNPq for their financial support to this project.

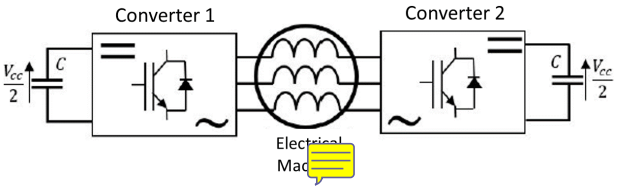

Fig. 1. Open-end winding configuration example [3].

Choosing a suitable pulse width modulation (PWM) technique can positively affect the overall behavior of the system. Multilevel configurations present redundant switching states that, when correctly used, can improve power quality, dynamics and losses distribution. Several PWM techniques have been reported over the last decades in order to achieve the best power quality and/or efficiency of the OEW configuration. Some are space vector based techniques such as the sub-hexagon in [7], others are carrier based, such as presented by [8], or hybrid, such as [9]. Finally, [10] shows that there is a correlation between OEW and FC converters, allowing the use of the centered space vector modulation (CSVPWM) with a state machine decoder to determine the best switching states.

In the work presented in this paper, carrier-based PWM techniques with three different carrier dispositions were analyzed: Phase Shifted (PS-PWM), Level Shifted with Phase Disposition (PD-PWM) and Level Shifted with Phase Opposition Disposition (POD-PWM). The point of comparison was the output energy quality and system performance was analyzed mainly through experimental results, with complementary simulations.

II. The Three-Level OEW Converter

The power circuit of the studied OEW system is illustrated in Fig. 2. Instead of the conventional delta or star connection, the load terminals are connected to a pair of two-level, three-phase, back-to-back converters, each one with its respective DC-link. In order to avoid the circulation of common-mode

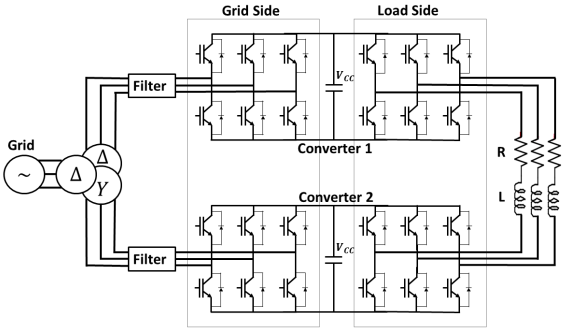

Fig. 2. Power circuit of the studied three-level OEW configuration

currents through the system, a transformer isolates the converters on the grid side. This configuration is capable of producing the same voltage outputs as a traditional three-level converter.

At the grid side, each converter presents an LCL filter in order to reduce the switching frequency harmonics. The 12-pulse transformer results in 5° and 7° harmonic mitigation when the converter demands power from the grid. The working dynamics of the system for this study consists of using the grid side as a power source to charge and control the ~~capacitive~~ bus at a constant voltage level. Each converter is controlled independently at the grid side, and voltage modulation is conducted using the traditional two-level space vector technique (SVPWM) [11].

At the load side, on the other hand, the voltage output is dependent of both converters that are then treated as a single three-level converter. ~~It is at this side that the modulation techniques under study are employed.~~

The experimental tests were conducted in a test bench built at the Energy Generation Laboratory of the Federal University of Itajubá - *campus* Itabira. Table I presents the system parameters, which were the same adopted in the simulation study. Command and control of the system were implemented and performed by a Texas Instruments TMS320F28335 digital signal processor. MatLab® was used to gather, process and present the data collected during the tests. Fig. 3 presents ~~images~~ of the experimental setup and its main components.

Simulation was performed using *PLECS*® with the same parameters of the test bench, allowing extrapolation of the experimental data to any condition.

TABLE I
EXPERIMENTAL SETUP PARAMETERS.

Parameters	*Values*
DC-link Total Voltage	200[V]
Load Resistance	10 [Ω]
Load Inductance	4 [mH]
Load Rated Active Power	1,25 [kW]
Load Maximum RMS Current	8,8 [A]
Load Power Factor	0,99
Output Voltage Switching Frequency	1200 [Hz]

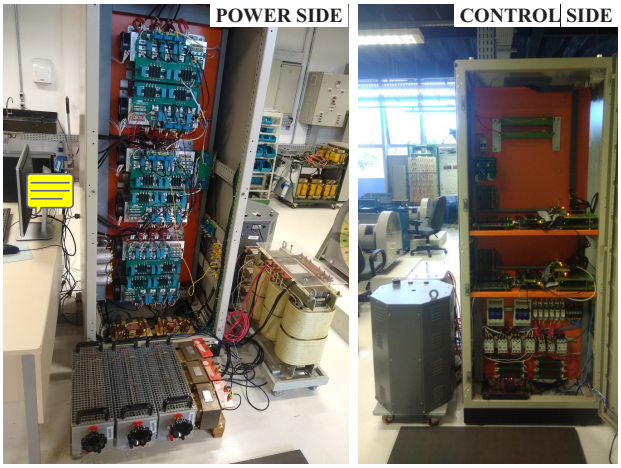

Fig. 3. Experimental setup configuration.

III. MODULATION TECHNIQUES

The choice of the modulation strategy directly interfere in the behavior and performance of the ~~energy~~ converter. As a result of advances in different multilevel converters topologies, studies on modulation strategies have come into evidence. Despite the complexity associated with the greater number of semiconductor devices to be controlled, the development of different techniques is directly related to the possibility of exploring additional switching states. As a result, they allow the power converter to operate at its best performance [1], [12].

Fig. 4 presents some of the most common modulation topologies for the multilevel configuration~~, each with~~ its own advantages, limits and ~~exclusivity of the given converter configuration~~.

Modulation methods can be classified according to the switching frequency (Hz) and if carrier-based, vector-based or others such as hybrid and selective harmonics elimination. Carrier-based strategies are widely used because they have a relatively simple implementation, attractive for operation with digital signal processors. Among them, two ~~strands~~ stand out:

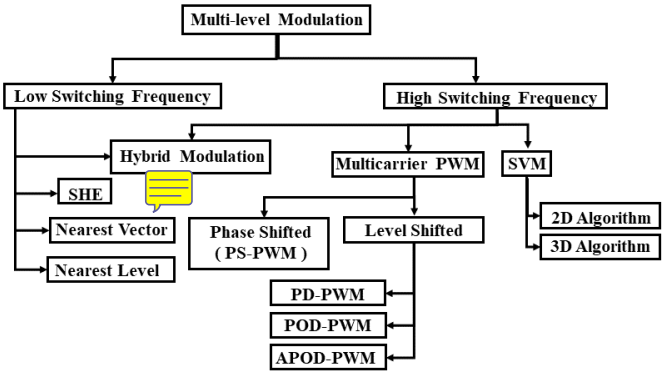

Fig. 4. Classification of modulation techniques for multilevel converters.

the first, uses phase shifted carriers (PS-PWM), and the second uses level shifted carriers (LS-PWM). The latter includes three different carrier dispositions: Phase Disposition (PD), Phase Opposition Disposition (POD) and Alternate Phase Opposition Disposition (APOD) [1], [13].

It was evidenced by [11], for two levels, and by [14], for the multilevel configuration, that the Centered Space Vector Pulse Width Modulation (CSVPWM) has similar output behavior to space vector techniques, through the addition of the correct zero sequence signal to a three-phase modulating signal. The basic operation of the CSVPWM is shown in the block diagram of Fig. 5. The zero sequence signal, added to the voltage reference, is obtained using equations (1), (2) and (3), which have the three-phase referential represented by $i \in (a, b, c)$ [14].

$$v_i{}' = v_i - \frac{\max(v_a, v_b, v_c) - \min(v_a, v_b, v_c)}{2} \tag{1}$$

$$v_i{}'' = \left[v_i{}' + (n-1)\frac{v_{dc}}{2}\right] \times \mathrm{mod}\ (v_{dc}) \tag{2}$$

$$v_i^* = v_i{}' + \frac{v_{dc}}{2} - \frac{\max(v_a{}'', v_b{}'', v_c{}'') - \min(v_a{}'', v_b{}'', v_c{}'')}{2} \tag{3}$$

In this study, an evaluation of the voltage output harmonic distortion was conducted for different carrier dispositions under the same circumstances, i.e., modulating signals. The analyzed strategies make use of $(n-1)$ carriers, being n the number of converter levels. In the three-level system, two carriers are compared to the three-phase modulating signals. One carrier is associated to converter 1 and the other to converter 2 (indicated in Fig. 3).

A. *Phase Shifted (PS-PWM)*

In this technique, carriers cover all modulating range and are phase shifted by an angle

$$\delta = \frac{2 \cdot \pi}{(n-1)} \tag{4}$$

For the three-level system, both converters are switched continuously at the carrier frequency and the voltage output is switched at twice this frequency. Fig. 6 illustrate its working principle.

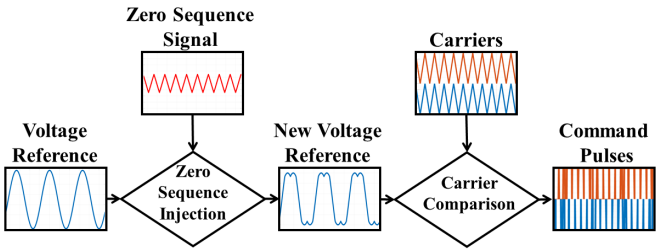

Fig. 5. Modulation block diagram.

B. *Phase Disposition (PD-PWM)*

In the PD-PWM, carriers are level shifted. Each carrier covers a $1/n$ fraction of the modulation range and are disposed with the same angular offset.

In the three-level OEW system, it means that each converter is switched during half the period of the modulating signal. The voltage output switching frequency is the same as the carrier, which is why it must have twice the frequency of the PS-PWM in order to allow a proper comparison between strategies.

Fig. 7 presents an example of PD-PWM operation.

C. *Phase Opposition Disposition (POD-PWM)*

The POD-PWM is also a level shifted strategy, with the difference that carriers below midpoint of the modulation range are disposed with a phase displacement of π rad regarding the ones above midpoint. This is depicted in Fig. 8.

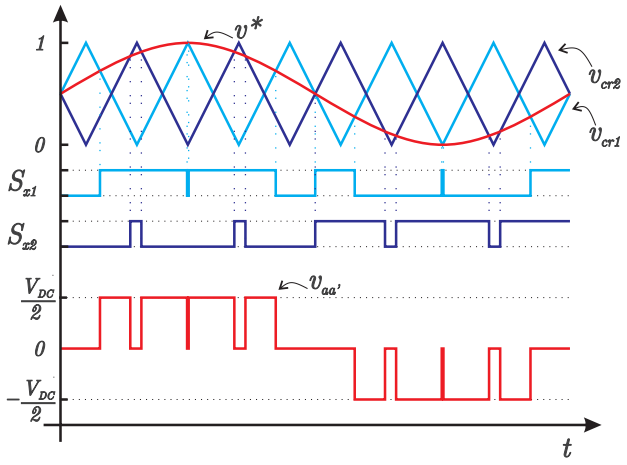

Fig. 6. Carrier and modulating signal for PS-PWM.

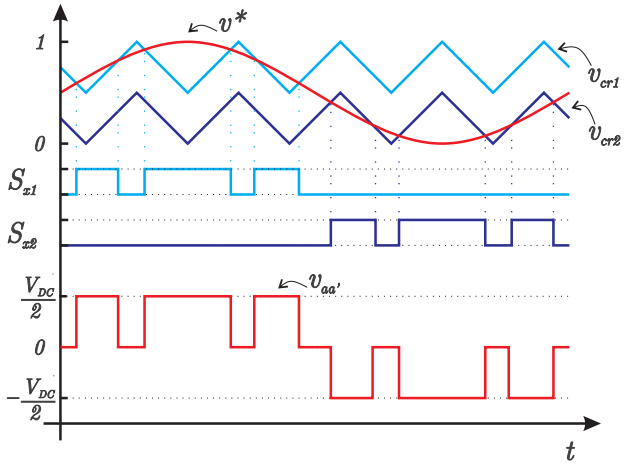

Fig. 7. Carrier and modulating signal for for PD-PWM.

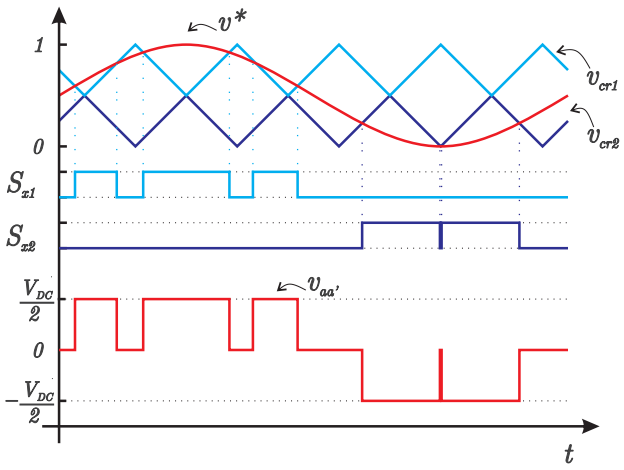

Fig. 8. Carrier and modulating signal for POD-PWM

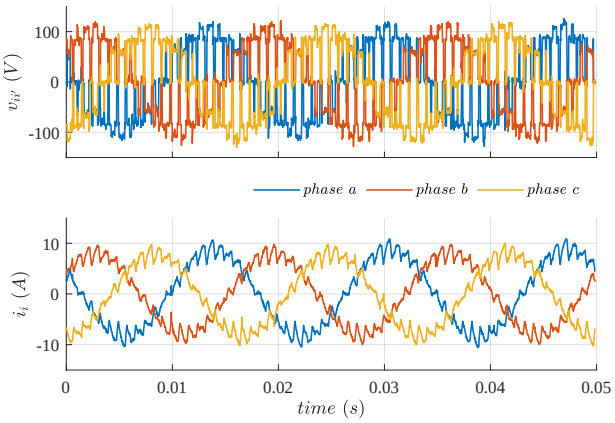

Fig. 9. Experimental results for the PS-PWM: three-phase voltages and currents.

IV. Testing and Results

In order to allow a proper comparison of the different carriers disposition methods, ~~testing~~ must be made under comparable circumstances. For all testing conditions, the RL load is fixed and the DC-links of both converters are controlled at the same level ($100V$) by their respective grid side bridges.

Also, the carrier frequencies for each technique must result in the same switching frequency in the voltage output. For that reason, the PS-PWM applies 600Hz carriers, while the level shifted strategies employ 1200Hz carriers. The first switching harmonic in the voltage output is then expected to be 1200Hz in all three analyzed strategies.

With those base conditions, the output voltages and currents were registered while the modulation index was swept over all the normal modulation range (overmodulation excepted). ~~Since there are different expressions for the modulation index calculation, it is relevant to present the one adopted in this work:~~

$$m_i = \frac{V^*}{V_{dc}} \frac{2}{\sqrt{3}} \tag{5}$$

being V^* the peak value of the output phase voltage, and V_{dc} the sum of both converters DC-link voltages.

All waveforms presented in this section were obtained through experimental ~~testing~~, using a modulation index $m_i = 1$~~,0~~ and compared based on spectral analysis.

A. PS-PWM Results

The PS-PWM resulting electrical variables can be seen in Fig. 9. The voltage waveform, presented in Fig. 9 (a), shows that there are abrupt transitions in amplitude, with a high frequency in the interval of a single switch, which characterizes a high (dV/dt) ratio. These are reflected on the current ripple, which is presented in Fig. 9 (b). The variables harmonic spectrum, depicted in Fig. 10, demonstrate that the first harmonic component of the switching frequency, at 1200Hz, is the most relevant one.

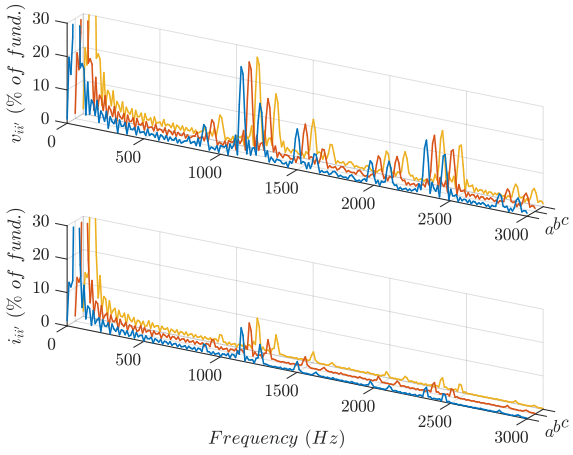

Fig. 10. Harmonic spectrum of the PS-PWM output voltages and currents.

B. PD-PWM Results

The voltage and current waveforms resulting from the PD-PWM can be seen in Fig. 11. Compared to the previous strategy, the voltages, shown in Fig. 11 (a), present transitions to closer levels, reducing dV/dt and resulting in a closer to sinusoidal waveform. This contributes to the reduction of the ripple present in the currents, observed in Fig. 11 (b). The improvement is reflected in the harmonic spectrum, presented in Fig. 12. The most relevant harmonic is at twice the switching frequency, as this modulation strategy is capable of mitigating the first switching harmonic at 1200Hz.

C. POD-PWM Results

The resulting waveforms obtained through the POD-PWM have shown to be closer to the PS-PWM and can be seen in Fig. 13. Voltage transitions occur between distant levels, leading to higher dV/dt and current ripple compared to PD-PWM. The first switching harmonic is not mitigated, as observed from the harmonic spectrum presented in Fig. 14.

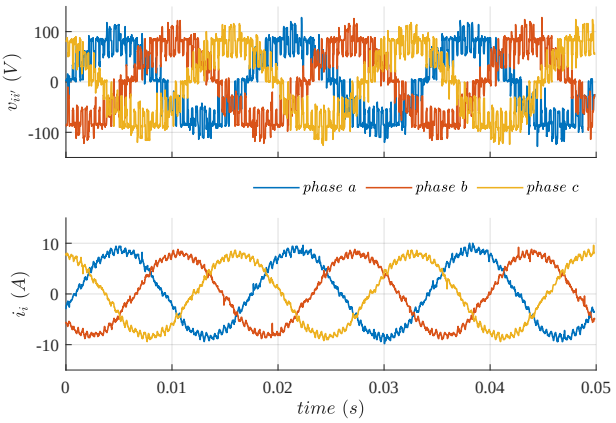

Fig. 11. Experimental results for the PD-PWM: three-phase voltages and currents.

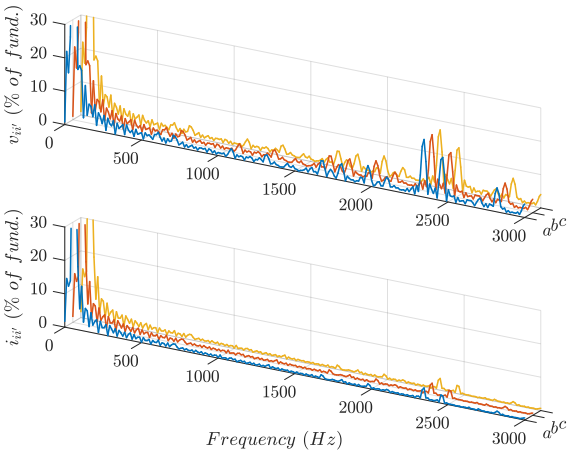

Fig. 12. Harmonic spectrum of the PD-PWM output voltages and currents.

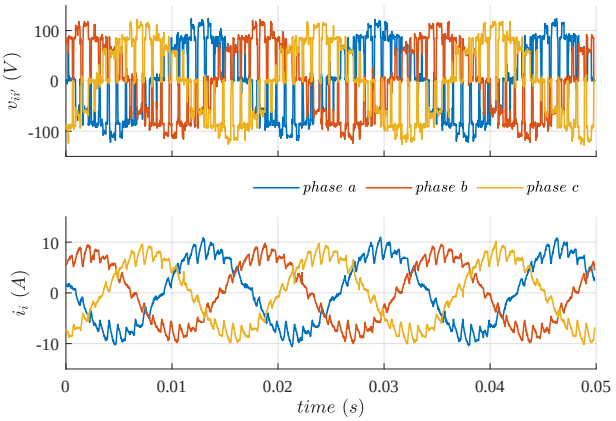

Fig. 13. Experimental results for the POD-PWM: three-phase voltages and currents.

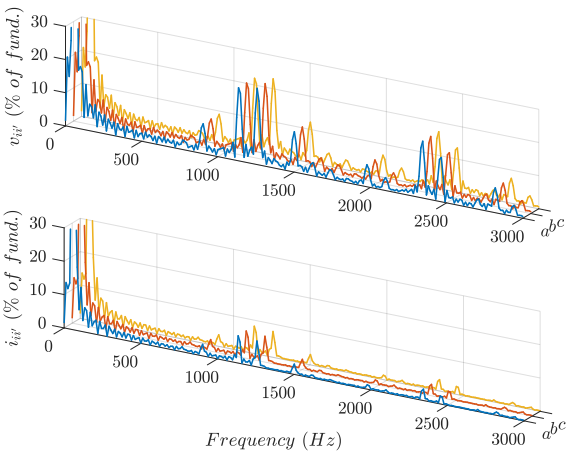

Fig. 14. Harmonic spectrum of the POD-PWM output voltages and currents.

D. Overall Performance

As a means to evaluate the overall performance of the strategies regarding output power quality, several modulation indexes were tested in the experimental setup. The *Total Demand Distortion* (TDD) [15] was calculated from collected results and plotted as the x points in Fig. 15, along with the system simulated data, represented by the continuous lines.

The analysis show that PS-PWM and POD-PWM produce similar outcomes, while PD-PWM presents the best performance for the entire modulation range.

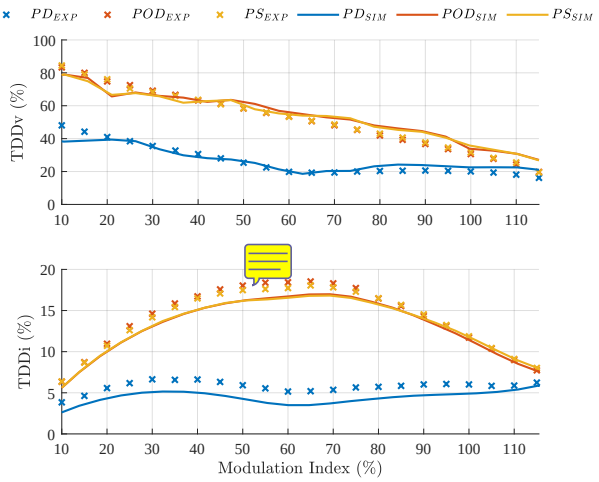

Fig. 15. Comparison of the total current demand distortion between the modulators as a function of the modulation index (experimental and simulated results).

V. Conclusion

This work analyzed the behavior of multilevel carrier-based modulation techniques with different carrier dispositions, applied to an open-end winding converter topology. The development of the study included the implementation and application of the PS-PWM, PD-PWM and POD-PWM strategies.

Based on experimental tests carried out in laboratory environment, the PD-PWM modulation strategy has presented superior performance in relation to the others, regarding the output voltage quality.

This work opens the path to expand future analysis of these modulation strategies applied to open-end winding topologies, including thermal losses, common-mode currents and different zero-sequence injection signals.

Acknowledgment

This work has been supported by the Coordination for the Improvement of Higher Education Personnel - Brazil (CAPES), the National Council for Scientific and Technological Development (CNPQ) project 408059/2021-4, the Minas Gerais Research Funding Foundation (FAPEMIG) projects APQ-01187-18 and APQ-00318-21.

References

[1] J. Rodriguez, L. G. Franquelo, S. Kouro, J. I. Leon, R. C. Portillo, M. A. M. Prats, and M. A. Perez, "Multilevel converters: An enabling technology for high-power applications," *Proceedings of the IEEE*, vol. 97, no. 11, pp. 1786–1817, Nov 2009.

[2] H. Stemmler and P. Guggenbach, "Configurations of high-power voltage source inverter drives," in *1993 Fifth European Conference on Power Electronics and Applications*, Sep. 1993, pp. 7–14 vol.5.

[3] V.Ricardi, "Acionamentos de geradores síncronos a Ímãs permanentes com bobinas abertas em sistemas de conversão de energia eólica," Master's thesis, Universidade Federal de Minas Gerais, 2018.

[4] M. Kwak and S. Sul, "Control of an open winding machine in a grid-connected distributed generation system," in *Conference Record of the 2006 IEEE Industry Applications Conference Forty-First IAS Annual Meeting*, vol. 5, Oct 2006, pp. 2576–2580.

[5] B. A. Welchko, "A double-ended inverter system for the combined propulsion and energy management functions in hybrid vehicles with energy storage," in *31st Annual Conference of IEEE Industrial Electronics Society, 2005. IECON 2005.*, Nov 2005, pp. 6 pp.–.

[6] F. F. V. Matos, H. d. O. Ramos, D. C. G. Rocha, R. M. da Silva, M. A. S. Mendes, and V. F. Mendes, "A multilevel wind power conversion system with an open winding squirrel cage induction generator," in *2015 IEEE 13th Brazilian Power Electronics Conference and 1st Southern Power Electronics Conference (COBEP/SPEC)*, Nov 2015, pp. 1–6.

[7] E. Shivakumar, K. Gopakumar, S. Sinha, A. Pittet, and V. Ranganathan, "Space vector PWM control of dual inverter fed open-end winding induction motor drive," *EPE Journal*, vol. 12, no. 1, pp. 9–18, 2002, publisher: Taylor & Francis.

[8] D. S. George and M. R. Baiju, "Decoupled random modulation technique for an open-end winding induction motor based 3-level inverter," in *2009 IEEE Symposium on Industrial Electronics & Applications*, Oct. 2009, iSBN: http://id.crossref.org/isbn/978-1-4244-4681-0 Publisher: Institute of Electrical & Electronics Engineers (IEEE). [Online]. Available: http://dx.doi.org/10.1109/ISIEA.2009.5356313

[9] G. d. A. Carlos, E. dos Santos, and C. Jacobina, "Hybrid PWM strategy for voltage source inverters feeding three-phase open-end-winding equipment," in *IECon 2012-38th Annual Conference on IEEE Industrial Electronics Society*. IEEE, 2012, pp. 459–464.

[10] F. F. V. Matos, M. A. S. Mendes, T. Meynard, and V. F. Mendes, "A generalized open-end winding conversion system using flying capacitor cells," *Electric Power Systems Research*, vol. 169, pp. 174–183, Apr. 2019, publisher: Elsevier BV.

[11] D. G. Holmes, "The general relationship between regular-sampled pulse-width-modulation and space vector modulation for hard switched converters," in *Proc. Conf. Record of the 1992 IEEE Industry Applications Society Annual Meeting*, Oct. 1992, pp. 1002–1009 vol.1.

[12] D. G. Holmes and T. A. Lipo, *Pulse Width Modulation for Power Converters: Principles and Practice*. IEEE, 2003.

[13] R. Teodorescu, *Grid Converters for Photovoltaic and Wind Power Systems*, 1st ed. IEEE, 2011.

[14] B. P. McGrath, D. G. Holmes, and T. Lipo, "Optimized space vector switching sequences for multilevel inverters," *IEEE Transactions on Power Electronics*, vol. 18, no. 6, pp. 1293–1301, Nov 2003.

[15] "IEEE Recommended Practice and Requirements for Harmonic Control in Electric Power Systems," *IEEE Std 519-2014 (Revision of IEEE Std 519-1992)*, pp. 1–29, Jun. 2014.